Uncertainty of measurement for large product verification: evaluation of large aero gas turbine engine datums

2016 Meas. Sci. Technol. 27 115003

(http://iopscience.iop.org/0957-0233/27/11/115003)

OPEN ACCESS
IOP Publishing
Measurement Science and Technology
Meas. Sci. Technol. **27** (2016) 115003 (12pp)
doi:10.1088/0957-0233/27/11/115003

Uncertainty of measurement for large product verification: evaluation of large aero gas turbine engine datums

J E Muelaner[1], Z Wang[1], P S Keogh[1], J Brownell[2] and D Fisher[2]

[1] Department of Mechanical Engineering, University of Bath, Bath, UK
[2] Rolls-Royce plc, Derby, UK

E-mail: j.e.muelaner@bath.ac.uk

Received 19 February 2016, revised 1 June 2016
Accepted for publication 8 July 2016
Published 22 September 2016

Abstract

Understanding the uncertainty of dimensional measurements for large products such as aircraft, spacecraft and wind turbines is fundamental to improving efficiency in these products. Much work has been done to ascertain the uncertainty associated with the main types of instruments used, based on laser tracking and photogrammetry, and the propagation of this uncertainty through networked measurements. Unfortunately this is not sufficient to understand the combined uncertainty of industrial measurements, which include secondary tooling and datum structures used to locate the coordinate frame. This paper presents for the first time a complete evaluation of the uncertainty of large scale industrial measurement processes. Generic analysis and design rules are proven through uncertainty evaluation and optimization for the measurement of a large aero gas turbine engine. This shows how the instrument uncertainty can be considered to be negligible. Before optimization the dominant source of uncertainty was the tooling design, after optimization the dominant source was thermal expansion of the engine; meaning that no further improvement can be made without measurement in a temperature controlled environment. These results will have a significant impact on the ability of aircraft and wind turbines to improve efficiency and therefore reduce carbon emissions, as well as the improved reliability of these products.

Keywords: large volume metrology, laser tracker, photogrammetry, datum structures

(Some figures may appear in colour only in the online journal)

1. Introduction

High accuracy large scale measurements are most commonly made using either a laser tracker or a photogrammetry system. Large structures with scales ranging from 1 m to 100s of metres with tolerances at or below 1 mm commonly rely on laser tracker measurements throughout the manufacturing process [1]. For example, assembly jigs and tooling are set using laser trackers [2], whilst large machine tools and robotic assembly systems are calibrated using laser trackers. Laser trackers are also used to align components during assembly [3], to check the form of emerging assemblies and to verify the form of finished products. Photogrammetry is typically used when it is beneficial to measure multiple coordinates simultaneously or when dynamic tracking of multiple coordinates is required.

A laser tracker is a large volume coordinate measurement device consisting of a laser distance measurement system mounted on a motorized gimbal arrangement with encoders to measure the pointing angles of the laser; azimuth and elevation [4]. A spherically mounted retroreflector (SMR) is used to return the laser beam to the laser tracker and to probe items to be measured. Since the SMR is a retroreflector the laser light is returned along a path parallel to the outgoing path, any

offset between these paths is detected by a position sensitive detector (PSD) within the laser tracker optics. The PSD provides feedback to the motors on the gimbal allowing the laser to be aligned with the optical centre of the SMR. This can also take place in real-time allowing the laser to track the SMR as it is moved [5]. The optical centre of the SMR's retroreflector is accurately aligned with the physical centre of its outer sphere so that the angular and distance measurements made by the laser correspond to the coordinates of the sphere's centre. The known radius of the sphere can then be used to offset these coordinates when probing surfaces with the SMR.

Laser trackers were originally developed for the calibration of industrial robots in the early 1980s [6]. It was quickly realised that they had considerably more potential and they replaced rapidly photogrammetry systems and theodolites [7] to become the standard measurement system for large scale high value products such as aircraft and spacecraft [8, 9]. Although there have been considerable advances in distance measurement techniques, miniaturization and practicality the basic functionality of a laser tracker remains unchanged. Although many of the examples considered in this article refer to laser trackers, the methods of propagating uncertainty from coordinate measurements through the optical tooling and datum structures to give uncertainty of actual measurements apply equally to measurements made using photogrammetry principles.

The way in which laser trackers and photogrammetry systems are used to measure tools, machines and products varies greatly depending on the requirements of the measurement. In some cases, such as the measurement of freeform surfaces, the target may be held against the surface to directly probe coordinates. More often, the commonly termed 'optical tooling' is used to hold the target at a known position relative to the feature being measured. This tooling typically features a three-point kinematic connection with magnetic retention to locate a spherically mounted target in at least one position. It also has other features to locate the tooling on the feature of the part being measured. Pins are often used to locate into holes and against edges. Kinematic mounts on a simple flat disk are used as common reference targets to locate different instrument stations relative to one-another and to monitor movement of structures.

Determining whether a measurement will be fit for purpose will normally involve some consideration of the uncertainty of the measurement with respect to the specification to be verified. Different methodologies can be used to do this, such as an uncertainty evaluation approach [10, 11] or a measurement systems analysis approach [12]. The relative merits of each approach have been discussed previously [13] and are therefore not described in this paper. Here an uncertainty evaluation approach is used.

Although further work is still required in some areas; for most practical purposes it is possible to model the uncertainty of laser tracker systems and networks. All of these models give some evaluation of the uncertainty in the coordinates of the SMR centre at each measured point. For some measurements this is sufficient. In many cases, however, the SMR is not directly able to measure the feature of interest. In these cases some intermediate tooling may be used to interface with the part being measured and some geometric calculation then carried out to infer the position of the feature being measured. This intermediate tooling is referred to as facility tooling or optical tooling. The optical tooling used and geometry fitting operations carried out can have a very significant impact on the uncertainty of measurements. A complete evaluation of uncertainty propagation through the measurement instrument, multi-instrument network, optical tooling and establishing the coordinate frame has not previously been considered in the literature. This paper addresses this gap in the knowledge.

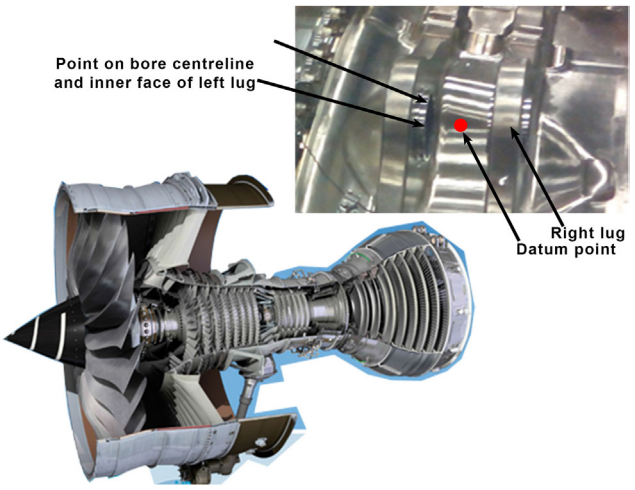

Figure 1. Aero Engine which was measured with close up of datum point constructed from measurements of lugs.

2. Large aero gas turbine engine measurement

A measurement process for a large aero gas turbine engine is used in this article to explain and validate the generic methods. In the following sections each stage in the propagation of uncertainty is considered sequentially; the instrument; multi-instrument networks; optical tooling and finally the datum structure used to locate the coordinate frame. In each section the generic methods are first described and the application of the methods to the engine measurement is then detailed.

In this section an overview of the engine measurement process is provided as background material. The measurement process involved positioning a laser tracker at three different locations in order to measure all of the datum features on the engine. In total there were 6 datum features, each consisting of a pair of lugs with a coaxial bore running through both lugs. These lugs are used to mount the engine on the aircraft wing. A datum point was constructed by first measuring a point on each lug at the intersection between the axis of the bore and the planar inner face of the lug. The datum point for each pair of lugs was then found by averaging the coordinates for these two constructed points, as shown in figure 1. In this way 6 datum points were constructed. A number of different types of tooling were used in the study to locate the bore and inner face, as described in section 5. The 6 datum points were then used to locate a coordinate frame according to a defined

datum structure as described in section 6. Subsequent measurements of features on the engine were made with respect to this coordinate system.

3. SMR uncertainty relative to instrument

A considerable amount of work has been carried out to enable the evaluation of uncertainty in laser tracker measurements [14–16]. This work includes traceability of the laser ranging system and modelling of geometric errors in the mechanical system used to direct the laser beam towards the SMR. This enables an understanding of the uncertainty of coordinates measured at the centre of the SMR from a single laser tracker location.

The most widely used model for the uncertainty of coordinates measured using a laser tracker considers each coordinate in a reference frame with the x-axis aligned along the direction of the laser. The uncertainty of the x-coordinate, Ux, is then dominated by the uncertainty in the distance measurement of the laser tracker while the uncertainties in the y and z coordinates, Uy and Uz, are dominated by the uncertainty in its angular measurement. Each of these is considered to be made up of a constant term and a range dependent term which increases linearly with distance from the laser tracker so that

$$Ux = A + Bx \tag{1}$$

$$Uy = Uz = C + Dx \tag{2}$$

where x is the distance from the laser tracker to the target, A is the constant uncertainty component for range dominated measurements, B is the range dependent uncertainty factor for range dominated measurements, C is the constant uncertainty component for angle dominated measurements, and D is the range dependent uncertainty factor for angle dominated measurements.

Once coordinate uncertainties have been calculated with respect to reference frames aligned along each beam path, coordinate transformations can be used to convert the coordinate uncertainties into a common coordinate system. This simple model is used by the American Society of Mechanical Engineers (ASME) for 'Performance Evaluation of Laser-Based Spherical Coordinate Measurement Systems' [17] and, subsequently, all the laser tracker manufacturers' specifications now use this model. A slightly simplified version of this model, in which the constant term is omitted for angle dominated uncertainties, is also used by some measurement software [18].

Slightly more complex models are used by some researchers and in experimental network adjustment software, for example, assigning different values to the vertical and horizontal angle encoders and including constants for systematic errors such as global scale error and dead path error [19]. This form of model is used in this study since it accounts for correlation between measurements resulting from the systematic errors.

Full 'virtual laser tracker' models, which explicitly consider all of the geometric errors, are sometimes used [20]. The main use of these more complex models is, however, during calibration. Once errors have been compensated it is usually sufficient to use one of the simpler models for coordinate uncertainty estimation and network adjustment. For the engine measurement, instrument locations were heavily constrained by the need to maintain multiple lines of sight to datum features on the engine and reference targets used to fit the multi-station measurements into a single datum frame.

A total of three laser tracker stations were positioned to the sides of the engine, approximately in the positive and negative y-direction from datum points. Uncertainty in the individual laser tracker measurements was therefore estimated by taking the manufacturer's maximum permissible error (MPE) for range in the y-direction and for angle in the x and z directions. At a range of 6 m the tracker MPE values at 3σ are therefore ± 31 μm along the axis of the laser beam and ± 75 μm in the two axes perpendicular to the laser beam (for which uncertainty is dominated by the angular encoders) [21]. It should be noted that throughout this paper where a standard deviation is calculated directly, this is expressed as a σ value. When a standard uncertainty resulting from uncertainty propagation is expanded by a coverage factor this factor is expressed as a k value.

4. Networked measurements

Models for the uncertainty in a single instrument, described previously, enable an understanding of the uncertainty of coordinates measured at a target from a single instrument location. The propagation of uncertainty through multi-station networks has also be researched using Monte Carlo simulation (MCS) techniques [18], which have been applied to industrial measurement software [22], and approaches based on the bundle adjustment techniques [23], well established in surveying and photogrammetry.

For the engine measurement, three instrument stations were used to measure all of the datum features on the engine. The uncertainty of the network measurements was determined by first calculating the azimuth, elevation and distance of each target from each instrument station. These were used to determine the Jacobian matrix of partial derivatives for the sensitivity of each measurement to uncertainty in sensor readings. The Jacobian matrix was combined with the instrument's uncertainty parameters to weight the 'trustworthiness' of each measurement, such that the weights are inversely proportional to the uncertainty. This was used to determine the coordinate uncertainties and covariances [24].

The positional uncertainties of the SMR's used to measure the V-groove tooling were first determined in this way. This used the current un-optimized network shown in figure 2(a) and assumed that 5 points were measured per V-groove with an angle of coverage of 80° for four of the datum points and 55° for the remaining two datum points, due to line-of-sight (LOS) constraints. The simulation also assumed that the tracker was operating according to the manufacturer's maximum permissible error (MPE) specifications.

The work now described sequentially following the propagation of uncertainty. In reality it was not possible to carry out

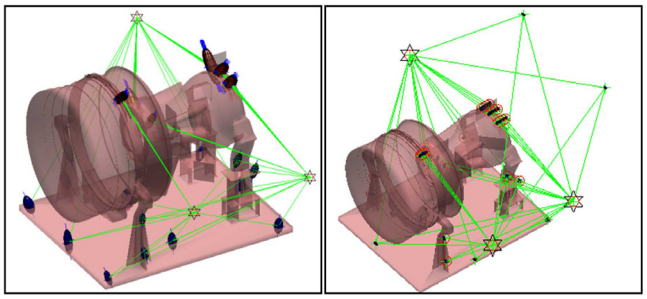

Figure 2. Tracker network configuration; original (left) and optimized (right).

optimization of the measurement network shown in figure 2(b) until after the design of improved tooling, described in section 5. The reason for this is that the design of the tooling determines the SMR positions required. The Tracker and reference target positions were then optimized to achieve line of sight whilst minimizing uncertainty.

5. Tooling uncertainty

Due to line of sight restrictions and bore diameter constraints, the direct measurement of bores may not be possible. Optical tooling is therefore often used. In this study 3 types of optical tooling are considered, which can be used to measure the position of a bore. Each of these has a shaft which locates into the bore and a shoulder which locates against the end face. The uncertainty due to the fit of the shaft in the bore is assumed to be negligible since it is dependent on the tolerance of the hole, which is outside the scope of this study. Due to the geometry of the bore and surrounding part it is not possible to directly place a single SMR at the intersection between the bore and the shoulder (the point of interest). Therefore each type of tooling also locates an SMR at 2 or more positions allowing the point of interest to be found.

The three types of tooling considered in this study are shown in figure 3; a V-groove design; a single sided vector bar and a symmetrical vector bar. The V-groove design has a V-groove profile revolved about the axis of the locating shaft, an SMR is placed in the groove at a number of locations and a circle is best fit through these points. The centre of the circle gives a point on the axis of the bore and the normal to the plane of the circle gives the direction vector of the axis, the known distance between the plane of the V-groove and the plane of the shoulder then give the position of the bore end fact along this vector. Vector bar tooling has 2 SMR location positions along the axis of the shaft and at known distances from the shoulder, locating the point of interest is then a simple offset from the SMR coordinates along the direction of the fitted line. This is the case for both types of vector bar. Where datums are constructed from pairs of points it may be possible to average coordinates without considering calibrated vector bar offsets. This is described for the engine measurement below.

Analysis of each type of generic bore measurement tool was carried out using Monte Carlo simulation (MCS), as evident in figure 4, to investigate the sensitivity to parameters involving the number and position of SMR locations. All

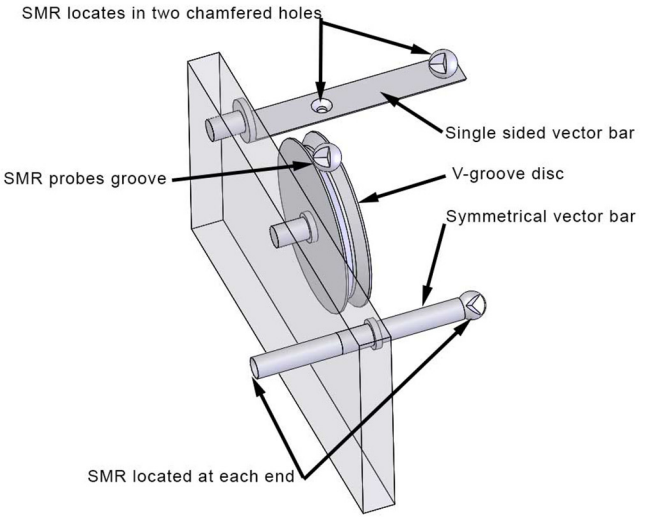

Figure 3. Three designs of optical tooling for bore measurement.

simulations used the same assumptions about the laser tracker and environmental uncertainties which result in an uncertainty of the SMR position of approximately 80 μm at 3σ.

Simulations showed that for V-groove tooling the radius of the points probed on the tooling has no significant effect on uncertainty. The angle of arc over which points were used to fit a circle was varied between 40° and 180°. The radius was set at 85 mm and 5 points were used to best fit a circle. This showed that when an arc of less than 120° is used the uncertainty increases significantly with an uncertainty approaching 1 mm for an arc of 40°, these results are summarised in figure 5 and agree with similar studies carried out previously [25].

A simulation was then carried out to investigate the effect of the number of points probed. The arc covered by the points was set at 80° and the radius at 85 mm. The number of points probed as incremented between 4 and 15 points with a total reduction in uncertainty over this range of values 0.22 mm–0.15 mm. This would, however, impact negatively on process time and a much more significant improvement could be achieved by increasing the arc covered, as shown previously.

For vector bar tooling the simulations show that for symmetrical designs the length has no effect on uncertainty while for single sided designs uncertainty increases strongly as length decreases, as shown in figure 6(a). Considering the single sided vector bar design it can be shown that the important design parameter is the position of the first SMR relative to the total vector bar length. This can be understood by expressing the distance from the measurement point to the first SMR as a percentage of the distance from the measurement point to the second SMR. The first SMR should be no more than 30% of the total length from the measurement point to achieve an optimal uncertainty value, as shown in figure 6(b). Achieving less than a 10% position would require very long vector bars, which are typically not practical. The results of these simulations are summarised in table 1.

It is also useful to note that if a vector bar can be accessed from both sides of the datum features, it is not necessary to calibrate the length of the bar or the thickness of the 'C' washer. Instead the midpoint between two surfaces can be

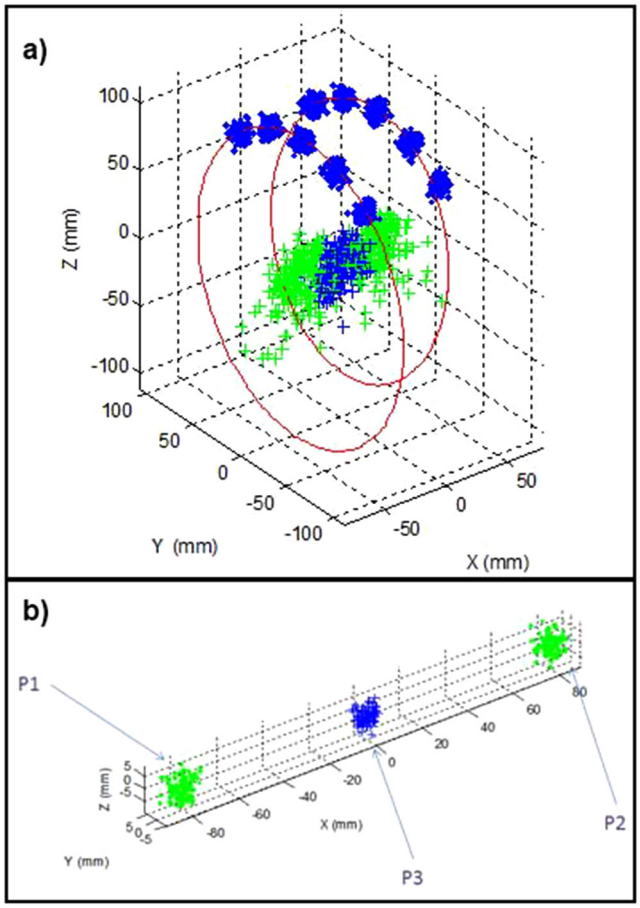

Figure 4. 3D Charts showing magnified errors from MCS's of optical tooling (a) V-groove tooling located in 2 lugs and used to find datum point between them; and (b) symmetrical vector bar tooling.

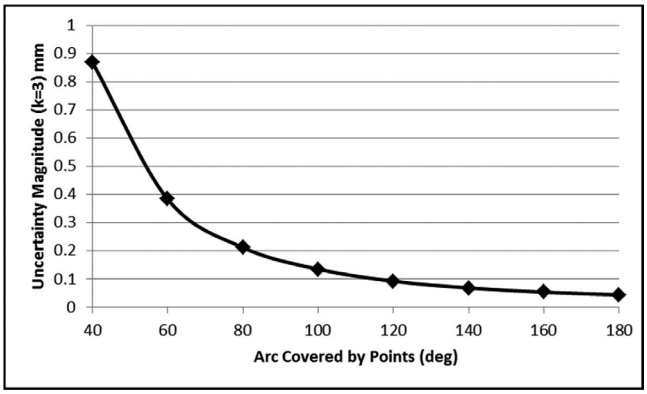

Figure 5. V-groove tooling simulation results for the effect of the arc covered on uncertainty of measurement.

found by reversing the bar. There is then no additional uncertainty due to calibration of the bar or thermal expansion of the bar. This can be proven analytically. Considering the vector bar, 'C' washer and part shown in figure 7, for which 8 measurements of an SMR are taken, it can be shown that the lengths of the vector bar and washer cancel out. The 8 measurements are taken at each end of the vector bar, with the vector bar in 4 positions. First the vector bar is located against the first datum face, with true position X_1, and measurements M_1

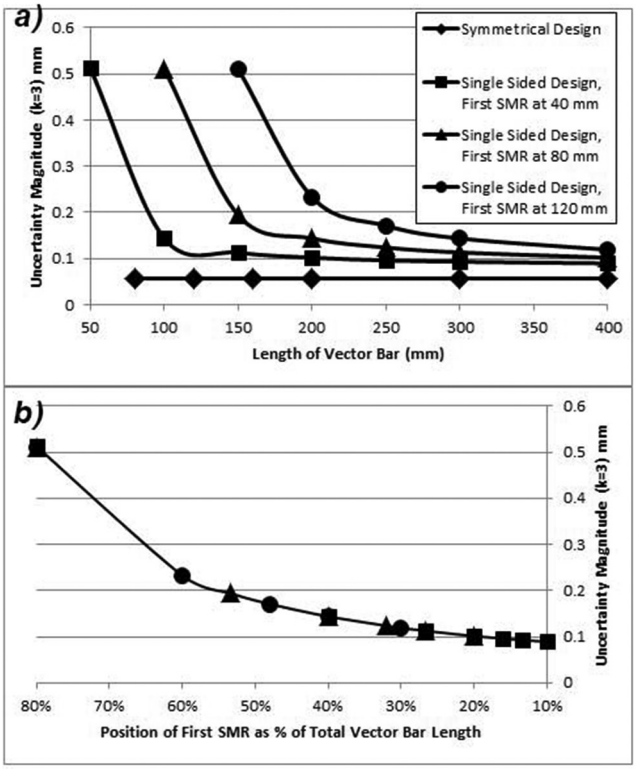

Figure 6. Results of MCS for vector bars; (a) single sided and symmetrical by total length; and (b) single sided by relative position of outer SMR.

and M_2 are taken at each end respectively. The vector bar is then moved along its axis to locate against the other datum face, with true position X_2, and measurements M_3 and M_4 are taken. The vector bar is then rotated by 180° and the process is repeated yielding measurements M_5 through M_8. The relations between the measured vector bar points (M_1 through M_8) and the 'C' washer points, X_1 and X_2, are given by

$$M_1 = X_1 + L_1 - L_4 - L_3 \tag{3}$$

$$M_2 = X_1 + L_1 + L_2 \tag{4}$$

$$M_3 = X_2 - L_1 - L_3 \tag{5}$$

$$M_4 = X_2 - L_1 + L_4 + L_2 \tag{6}$$

$$M_5 = X_1 + L_1 - L_4 - L_2 \tag{7}$$

$$M_6 = X_1 + L_1 + L_3 \tag{8}$$

$$M_7 = X_2 - L_1 - L_2 \tag{9}$$

$$M_8 = X_2 - L_1 + L_4 + L_3 \tag{10}$$

The average of the measured points is equal to the midpoint between the two datum surfaces and the dimensions of the tooling do not need to be known since summation of equations (3) through (10) shows that the lengths L_1, L_2, L_3 and L_4 cancel to yield:

$$\frac{X_1 + X_2}{2} = \frac{\sum_{i=1}^{8} M_i}{8} \tag{11}$$

Table 1. Summary of bore measurement tool MCS.

Type	% of SMR uncertainty (%)
5 point circle, 40° coverage	1088
5 point circle, 80° coverage	265
5 point circle, 180° coverage	55
2 point symmetrical vector bar	70
2 point single sided vector bar with first SMR at 30% of total length	150

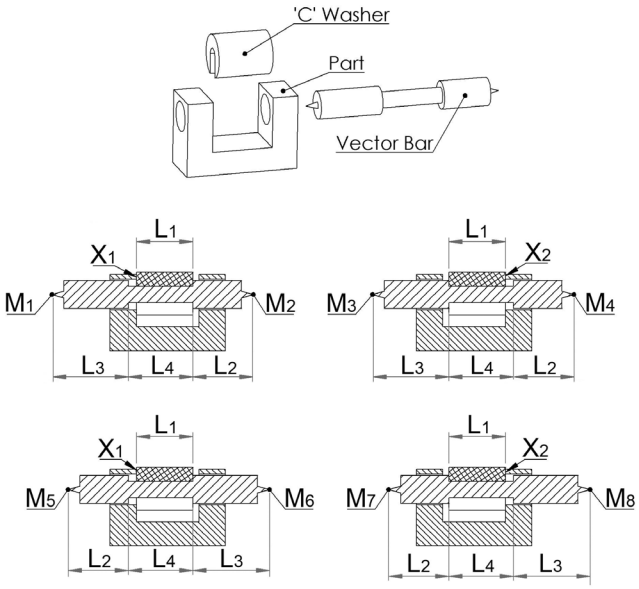

Figure 7. Vector bar reversal to obtain midpoint.

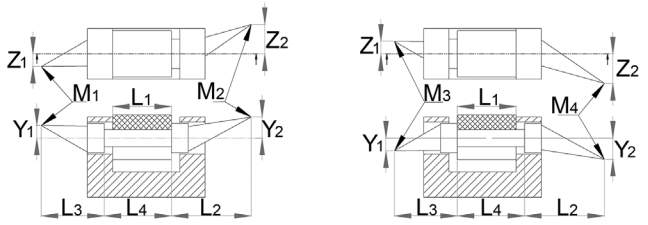

Figure 8. Vector bar rotation to cancel alignment errors.

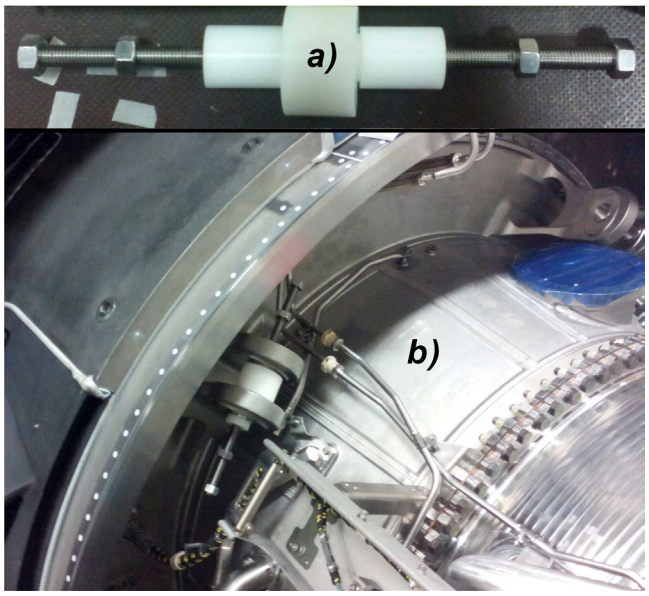

Figure 9. Early rapidly reconfigurable tooling; (a) the prototype; (b) testing on engine.

This approach has the added advantage of cancelling errors in shaft alignment if the vector bar is also rotated 180° between each measurement position. This is illustrated in figure 8 where alignment errors are present in the shaft and equations (3)–(6) remain true for the x-position of the datum.

In this case the average errors in the y and z positions are given by

$$\overline{E}_y = Y_1 + Y_2 - Y_1 - Y_2 = 0 \tag{12}$$

$$\overline{E}_z = Z_1 + Z_2 - Z_1 - Z_2 = 0 \tag{13}$$

Using multiple locations of the vector bar will also reduce uncertainty in the tightening of the washer against the datum faces through averaging. In fact it is also possible to find the midpoint with only two measurements; M_1 and M_8, using a single sided vector bar. This would save time, but would increase uncertainty, as this measurement process would not cancel errors in shaft alignment or average uncertainty due to tightening.

The engine measurement baseline process used V-groove tooling, which due to line-of-sight constraints, was proved over an arc of between 40° and 80° depending on which datum point it was applied. From the above analysis it is clear that this will result in considerably increased uncertainty of measurement compared to other tooling options. Even in the best case of an 80° arc this would result in an uncertainty of around 0.2 mm compared with around 0.05 mm for symmetrical vector bars of any length and 0.1 mm for single sided vector bars of sufficient length. In order to check the usability of the symmetrical vector bar, in terms of operator access to the engine datums and line of sight, a series of prototypes were constructed. Early prototypes were designed to be rapidly adjustable on-site so that the length could be adapted to achieve the required lines of sight while ensuring it could still be easily inserted into the engine datums by an operator. Lengths of stud were combined with nuts to enable the length of the vector bars and therefore the location of SMR mounts to be adjusted in this way. An example of one of these early prototypes is shown in figure 9.

The initial symmetrical vector bar design was found to be suitable for use on 2 datum points while one required a very short double sided, but not symmetrical, design placed through each lug in turn and with one SMR visible between the lugs and one on the outside as shown in figure 10.

For the 3 tail mount datums, double sided vector bars were not possible due to line of sight restrictions. It was therefore decided to use a single sided vector bar with both SMR's mounted rear of the tail mounts, as shown in figure 11.

Following initial tests MKII tooling designs were created as shown in figures 10–12. These were optimized for stiffness,

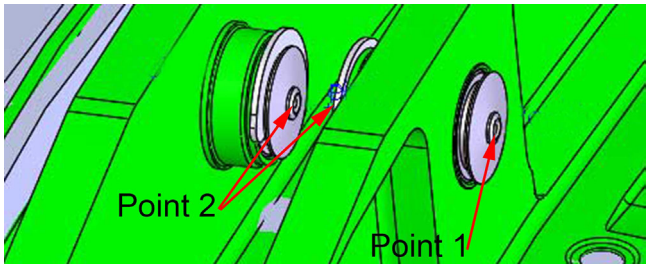

Figure 10. Short double sided design.

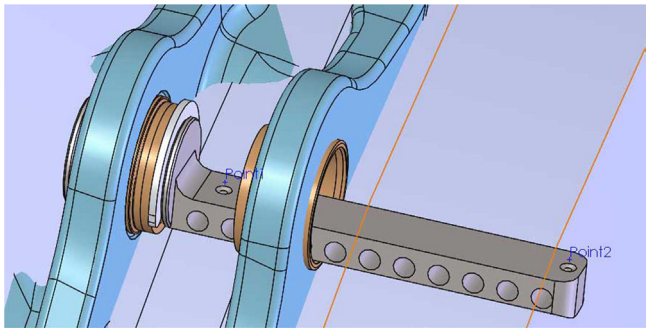

Figure 11. Single sided vector bar design for tail mount datums.

weight, accessibility and line-of-sight. Finite element analysis was used to determine deflection under gravity loading which was found to be less than 10 μm in all cases. These designs were then rapid prototyped using 3D printing and tested on the engine.

6. Coordinate frame uncertainty

A datum structure defines the way in which features on the part are used to locate a coordinate frame, also called a datum frame. Datum structures typically involve some form of '3-2-1' alignment in which the primary datum controls 3° of freedom, the secondary datum controls 2° of freedom and the tertiary datum controls the final degree of freedom. The simplest and most common form of 3-2-1 alignment involves datums consisting of 3 nominally perpendicular planes. Consider an example where these planes are arranged so that their surface normals point in the x-direction for the primary datum, the y-direction for the secondary datum and the z-direction for the tertiary datum. In this case; 3 points are measured on the primary datum plane to control translation in the x-direction and rotation about the y and z axes; 2 points are measured on the secondary datum plane to control translation in y and rotation about rotation about x; and finally one point is measured on the tertiary datum to control translation in z.

The uncertainty in each of the 6° of freedom results from the uncertainties of the individual measurements and their sensitivity coefficients. Obtaining a full analytical model for these sensitivity coefficients can be challenging for complex datum frames and will normally involve some simplifying assumptions.

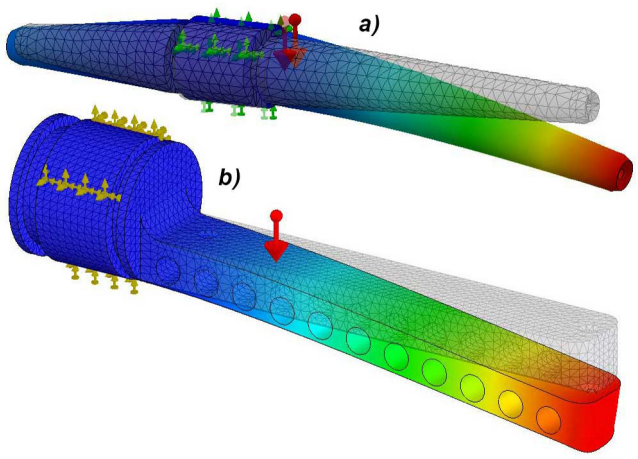

Figure 12. Tooling FEA; (a) thrust lugs; (b) tail mounts.

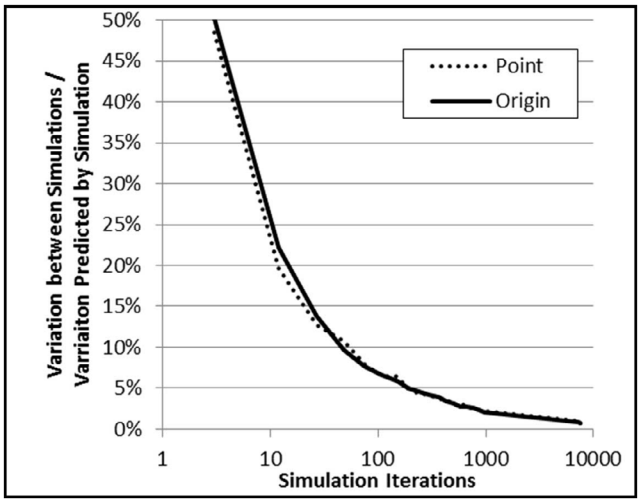

Figure 13. Effect of iterations of Monte Carlo simulation.

The number of iterations required to achieve some predefined level of accuracy for a MCS cannot be determined without adaptively trying different MCS's [26]. A convergence study was therefore carried out to determine the iterations required to give an appropriate accuracy for this type of MCS. The study carried out 100 simulations at each iteration level to determine the variation between simulation results as a fraction of the predicted simulation results. 50 iteration levels were simulated with values between 3 iterations and 7500 iterations. The study was applied to the simple simulation of a single coordinate measurement and fitting a datum frame to three planes using a 3-2-1 alignment. The results, summarised in figure 13, showed that the complexity of the simulation had no effect on the iteration levels required and that there is an exponential relationship between simulation iterations and simulation precision. To achieve a precision of better than 5% required approximately 200 iterations while to achieve better than 1% required over 7000 iterations. There is no reason to expect significant bias in a well-designed simulation and therefore the precision should represent the accuracy. The relationship between simulation iterations and simulation precision is given by

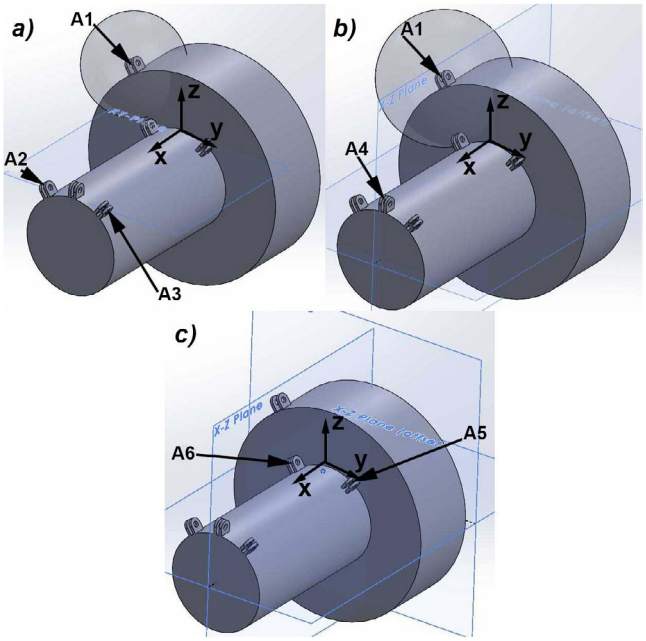

Figure 14. Datum structure for aero engine (a) Location of *X*–*Y* Plane constraining translation in the *z*-direction and rotation about the *x* and *y* axes. (b) Location of the *X*–*Z* Plane constraining translation in the *y*-direction and rotation about the *z* axis. (c) Location of the *Y*–*Z* Plane constraining translation in the *x*-direction.

$$\sigma_i/\sigma_s = 0.76 \cdot i^{-0.512} \tag{14}$$

where σ_s is the standard deviation in the coordinates as predicted by the simulation and σ_i is the standard deviation in σ_s for multiple simulations run with i iterations. σ_i/σ_s is therefore a measure of simulation precision.

For the engine measurement the datum measurement process was a 3-2-1 alignment involving six datum points. Each datum point is constructed from 4 datums features; the 2 nominally coaxial bores running through a pair of lugs; and the inner faces of these lugs, as shown in figure 1. For each lug a point is first constructed at the intersection of the bore axis and the inner face. The datum point is then found as the midpoint of the two constructed points. The uncertainty of these tooling inferred points was discussed in the preceding section.

The datum points were then used to construct a coordinate system, as shown in figure 14, by fitting three planes:

(a) The *X*-*Y* Plane is constructed first by fitting a plane through *A*2 and *A*3 tangent to a sphere of radius 660.955 mm about *A*1. This constrains translation in the *z*-direction, rotation about *x* and rotation about *y* (*z*, *i* and *j* respectively).

(b) The *X*-*Z* Plane is constructed next by fitting a plane perpendicular to the *X*-*Y* plane through *A*4 and tangent to a sphere of radius 611.64 mm about *A*1. This constrains translation in the *y*-direction and rotation about *z* (*y* and *k* respectively).

(c) Finally the *Y*-*Z* Plane is constructed by fitting a plane perpendicular to the *X*-*Y* and *X*-*Z* planes and passing through a point midway between *A*5 and *A*6, constraining the remaining degree of freedom; translation in the *x*-direction.

The propagation of uncertainty from the tooling inferred points through the datum structure gives an uncertainty in position and orientation of the coordinate system.

Assuming approximately equal uncertainty for each datum point, the uncertainty in the translation of the coordinate system in each axis can be estimated as the average uncertainty for the points used to locate the plane divided by the root of the number of points:

$$UC_x = \frac{UA5_x + UA6_x}{2 \cdot \sqrt{2}} \tag{15}$$

$$UC_y = \frac{UA1_y + UA4_y}{2 \cdot \sqrt{2}} \tag{16}$$

$$UC_z = \frac{UA1_z + UA2_z + UA3_z}{3 \cdot \sqrt{3}} \tag{17}$$

where UC_x is the uncertainty in the position of the coordinate system in the x direction and $UA5_x$ is the uncertainty of the datum point *A*5 in the x direction and so forth.

The uncertainty in the orientation of the coordinate system about each axis can be approximated by projecting the points that constrain this rotation onto the plane perpendicular to the axis and then considering the uncertainty in the angle of this line.

Following this approach; i is approximated as the elevation angle of a line projected onto the nominal *Y*-*Z* plane between the *Y*-*Z* coordinates of *A*1 and *A*3; j is approximated as the elevation angle of a line projected on the nominal *X*-*Z* plane between the *X*-*Z* coordinates of *A*1 and the averaged coordinates of *A*2 and *A*3; and k is approximated as the azimuth angle of a line projected onto the nominal *X*-*Y* plane between the *X*-*Y* coordinates of *A*1 and *A*4. The nominal angles are therefore given by

$$i = \tan^{-1}\frac{A1_z - A3_z}{A3_y - A1_y} \tag{18}$$

$$j = \tan^{-1}\frac{A1_z - \left(\frac{A2_z + A3_z}{2}\right)}{\left(\frac{A2_x + A3_x}{2}\right) - A1_x} \tag{19}$$

$$k = \tan^{-1}\frac{A1_y - A4_y}{A1_x - A4_x} \tag{20}$$

According to the law for the propagation of uncertainty [10] the uncertainties in these nominal angles are given by

$$Ui = \sqrt{\left(\frac{\partial i}{\partial A1_y}\right)^2 UA1_y^2 + \left(\frac{\partial i}{\partial A1_z}\right)^2 UA1_z^2 + \left(\frac{\partial i}{\partial A3_y}\right)^2 UA3_y^2 + \left(\frac{\partial i}{\partial A3_z}\right)^2 UA3_z^2} \tag{21}$$

$$Uj = \sqrt{\left(\frac{\partial j}{\partial A1_x}\right)^2 UA1_x^2 + \left(\frac{\partial j}{\partial A2_x}\right)^2 UA2_x^2 + \left(\frac{\partial j}{\partial A3_x}\right)^2 UA3_x^2 + \left(\frac{\partial j}{\partial A1_z}\right)^2 UA1_z^2 + \left(\frac{\partial j}{\partial A2_z}\right)^2 UA2_z^2 + \left(\frac{\partial j}{\partial A3_z}\right)^2 UA3_z^2} \quad (22)$$

$$Uk = \sqrt{\left(\frac{\partial k}{\partial A1_x}\right)^2 UA1_x^2 + \left(\frac{\partial k}{\partial A4_x}\right)^2 UA4_x^2 + \left(\frac{\partial k}{\partial A1_y}\right)^2 UA1_x^2 + \left(\frac{\partial k}{\partial A4_y}\right)^2 UA4_x^2} \quad (23)$$

Deriving the partial derivatives analytically and substituting these into equation (21) would result in a very unwieldy equation and is not necessary. Instead the numerical value for each partial derivative can be calculated at the nominal angle using the finite difference method.

Although this analytical uncertainty evaluation provides a reasonable order of magnitude estimate for the uncertainty it makes a number of assumptions, which has an influence on the accuracy. Most importantly, the way in which optical tooling scales the uncertainty of individual laser tracker measurements is highly directional and this has not been modelled here. A Monte Carlo simulation (MCS) approach described in the following section can be applied to avoid these deficiencies by considering the entire propagation of uncertainty through the measurement process.

7. Combined uncertainty of measurements with respect to coordinate system

The preceding sections have provided relevant analysis of the propagation of uncertainty through individual coordinate measurements, multi-station networks, vector bar tooling and datum frames. This section will show how an uncertainty budget can be used to combine the uncertainties derived analytically in the previous sections with additional uncertainties present when measurements are made with respect to the datum frame. The following section will then present a more accurate approach using Monte Carlo simulation (MCS) of the entire measurement process.

The simplest approach to considering the uncertainty of coordinates measured with respect to the datum frame is to consider the worst case where coordinates are measured at the edges of the part furthest from the datum frame's origin. In this case the measured coordinate's uncertainty results from both positional and angular uncertainty in the datum frame. For each axis the coordinate's uncertainty due to the datum frame is given by the datum frame's positional uncertainty in that axis combined in quadrature with the product of the tangent of the rotation uncertainty for the other two axes multiplied by the maximum distance from the origin to the edge of the part. For example, the maximum uncertainty in the x-direction is given by

$$UM_x = \sqrt{(UC_x)^2 + (L_y \tan U_k)^2 + (L_z \tan U_j)^2} \quad (24)$$

where UC_x is the uncertainty of the datum frame in the x-direction, L_y is the greatest distance in y from the datum frame to a point on the part, U_k is the uncertainty of the datum frame in rotation about the z-axis, L_z is the greatest distance in z from the datum frame to a point on the part and U_j is the uncertainty of the datum frame in rotation about the y-axis.

The uncertainty due to thermal expansion of the part is simply the product of the dimension of the part, the coefficient of thermal expansion (CTE) for the part material and the uncertainty in the temperature of the part during measurement. Normally, this is represented in an uncertainty budget as the uncertainty in the temperature stated as a source of uncertainty and the product of the part dimension and CTE stated as the corresponding sensitivity coefficient. This represents an approximation since in typical conditions there will be a temperature gradient and the product may be an assembly with components having different CTE's.

Applying an analytical uncertainty evaluation will involve combining the uncertainties into an uncertainty budget. Typically, uncertainty budgets consider the factors influencing 1D measurements. For coordinate measurements used to construct a datum frame with respect to which further coordinate measurements are made some modification to the uncertainty budget structure are required.

For this engine measurement it was assumed that the primary tracker station measures datums $A1$, $A2$, $A4$ and $A6$ and that a secondary station locates its-self to the primary station and then measures datums $A3$ and $A5$. Due to the orientation of the trackers the SMR coordinate uncertainties can be estimated by taking the manufacturers maximum permissible error (MPE) for range in the y-direction and for angle in the x and z directions [21]. At a range of 6 m the tracker MPE values at 3σ are therefore ± 31 μm in range and ± 75 μm in angle. To allow for the environmental conditions and repeatability of location in the tooling these values were doubled and targets measured from the secondary station multiplied by 1.3 to account for the uncertainty in the location. These factors were determined from experience of the use of the instruments in the actual environment and suitable factors for other environments should be determined experimentally.

Using the facility tooling scaling factor derived from the sensitivity studies for the current tooling the datum point uncertainties can also be derived. Using these datum point uncertainties the uncertainty of the datum structure in both position and orientation can also be calculated. Uncertainty due to manufacturing tolerances of the tooling was assumed to be negligible.

The thermal expansion of the engine was calculated assuming a 3σ temperature variation of ± 4 °C and a CTE of 22 μm m^{-1} °C^{-1}. The deformation due to gravity loads and tooling clamping forces acting on the engine have been ignored due to the extreme difficulty of estimating these for a complex aero engine.

Table 2. Combined uncertainty budget (analytical) for current process.

Datum point	SMR uncertainty at $k = 3$ (mm)			Facility tooling arc coverage (°)	Facility tooling scaling factor	Datum point uncertainty at $k = 3$ (mm)		
	x	y	z			x	y	z
*A*1	0.150	0.062	0.150	80	2.67	0.401	0.167	0.401
*A*2	0.150	0.062	0.150	80	2.67	0.401	0.167	0.401
*A*3	0.195	0.081	0.195	80	2.67	0.522	0.217	0.522
*A*4	0.150	0.062	0.150	80	2.67	0.401	0.167	0.401
*A*5	0.195	0.081	0.195	60	4.76	0.928	0.386	0.928
*A*6	0.150	0.062	0.150	60	4.76	0.714	0.297	0.714
					Datum translation	0.580	0.118	0.255
					Datum rotation (°)	0.027	0.010	0.005
					Max dist. from origin	2360	1577	2760
					Resulting uncertainty at edge	0.753	0.230	0.883
					Thermal expansion	0.208	0.139	0.243
					Combined uncertainty	0.781	0.269	0.916
					Magnitude		1.223	

The complete combined uncertainty calculation is summarized in table 2 showing a combined uncertainty magnitude of 1.223 mm for measurements at the edge of the engine. This analytical evaluation of the coordinate system uncertainty does not fully account for the 3D propagation of uncertainty; it also makes a number of gross assumptions as described previously. A more rigorous evaluation is provided by a numerical MCS of the complete measurement process.

8. Combining uncertainty using Monte Carlo simulation

In general the complete process of evaluating and optimizing measurement uncertainty for large measurements involving multi-instrument networks, optical tooling and datum frames will involve the following steps:

1. Identify datum structure, datum features on CAD model and approximate instrument stations. Key measurements may also be considered at this stage.
2. Initial design of tooling for datum feature measurement (and key measurement features if considered at this stage).
3. Network optimization (instrument locations and reference network, also iteration of tooling design)

   a. Objective function defined; may be datum frame position and orientation or it may be key measurements with respect to the datum frame.
   b. Simulate instrument measurements.
   c. Simulate network fitting.
   d. Simulate tooling fitting.
   e. Simulate datum location.
   f. Simulate measurements (optional).
   g. Iterate datum structure and/or tooling design if required.

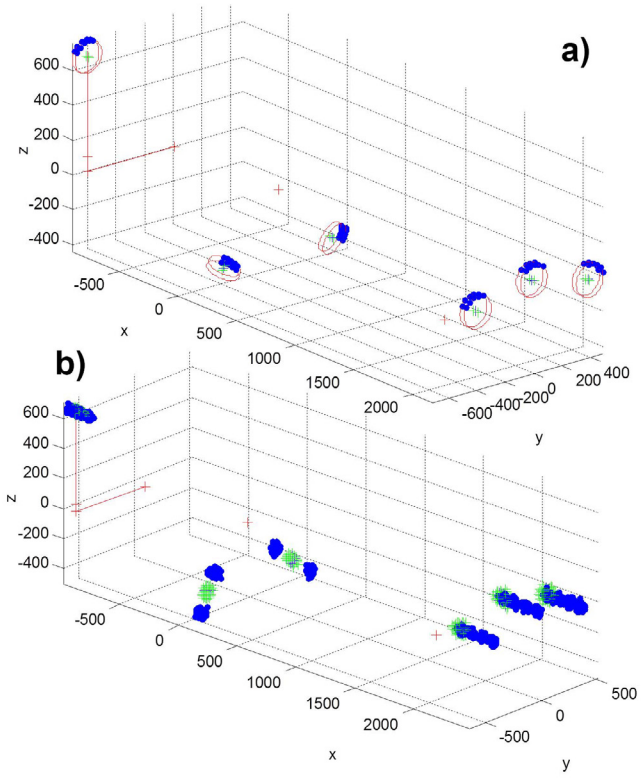

Figure 15. Simulations for measurement process using (a) current process with V-groove tooling, and (b) optimized process with vector bar tooling.

In order to obtain an improved estimate for the uncertainty of the engine measurement a MCS of the complete process was carried out. This involved first simulating the laser tracker network and the resulting SMR uncertainties. The SMR uncertainties were then used as seed uncertainties to simulate the uncertainty in best-fitting circles to locate the centres of the V-groove tooling, to find the datum points midway between

Table 3. Combined uncertainty budget (MCS) for current process.

Datum point	SMR uncertainty at $k = 3$ (mm)			Facility tooling arc coverage (°)	Facility tooling scaling factor	Datum point uncertainty at $k = 3$ (mm)		
	x	y	z			x	y	z
*A*1	0.064	0.127	0.147	80	N/A	0.562	1.058	1.008
*A*2	0.058	0.134	0.177	80	N/A	0.575	0.991	1.483
*A*3	0.069	0.198	0.192	80	N/A	0.560	0.991	0.840
*A*4	0.063	0.139	0.197	80	N/A	0.557	1.083	1.131
*A*5	0.064	0.189	0.186	60	N/A	0.579	0.190	0.363
*A*6	0.057	0.108	0.167	60	N/A	0.608	0.190	0.950
					Datum translation	0.561	0.542	0.596
					Datum rotation (deg)	0.061	0.016	0.012
					Max dist. from origin	2360	1577	2760
					Resulting uncertainty at edge	1.018	0.739	1.900
					Thermal expansion	0.208	0.139	0.243
					Combined uncertainty	1.038	0.752	1.915
					Magnitude		2.305	

pairs of V-groove locations, and to fit the datum structure to the datum points, as illustrated in figure 15. MCS was used with 80 000 iterations.

The results of the MCS are given in table 3. *A*5 and *A*6 locate the datum structure in the x-direction, but have particularly high uncertainty in the x-direction due primarily to the instability in fitting a circle to the V-groove in this direction. Similarly *A*1, *A*2 and *A*3 locate the datum structure in the z-direction, but have particularly high uncertainty in the z-direction for the same reason. So we can see that the uncertainties inherent in the V-groove tooling design happen to orientate themselves in particularly problematic directions. The datum point uncertainties can also be input to the analytical uncertainty model to verify this.

An improved process was designed using vector bar tooling, as described previously. The positon of the laser trackers and reference targets were then optimized using laser tracker network optimization algorithms [24].

The MCS described above was then repeated for this optimized process. The results of all three uncertainty evaluations are shown in figure 16. In the figure the uncertainty of individual SMR coordinates is represented by the 'Mean Tracker Network' and the uncertainty of the tooling inferred datum points is represented by the 'Mean Datum Points'. The propagation of uncertainty through the datum structure is then shown first for the location of the coordinate system origin, referred to as 'Datum Translation', and then adding to this the effect of angular uncertainty in the datum frame on coordinates measured at the edges of the engine, 'Datum Translation and Rotation'. Finally the effect of thermal expansion on whole engine measurements is considered.

The errors in the analytical evaluation can be seen to originate in the location of datum points which can be attributed to the directional uncertainty induced by the V-groove tooling happening to orientate themselves in particularly problematic directions. It is clear that the biggest improvement is

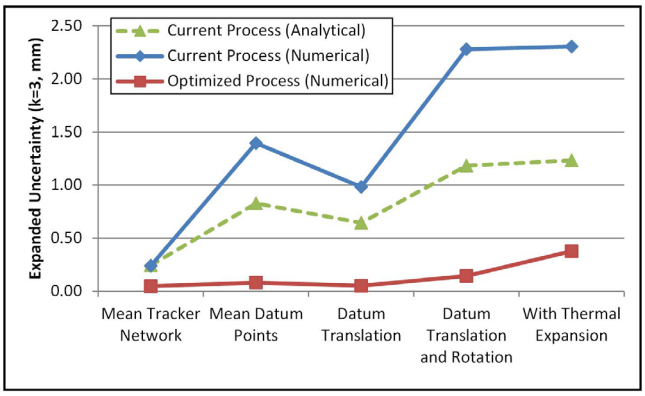

Figure 16. Propagation of uncertainty for current and optimized measurement processes.

predicted to result from the improved tooling used to locate the datum points. Subsequent differences in datum translation and rotation result directly from changes in the network and tooling since no changes have been made to the engine datum structure. It is also clear that for the current process thermal expansion is negligible when compared to other uncertainties while for the improved process thermal expansion is expected to become the dominant component of uncertainty.

9. Conclusions

A methodology for the evaluation and optimization of uncertainty in large scale industrial measurements has been developed. This addresses the weaknesses in current methods by providing a rigorous assessment of the effects of optical tooling and datum alignment. This paper therefore presents for the first time a complete evaluation of the uncertainty of a large scale industrial measurement process, in this case using a laser tracker. Generic analysis and design rules are

demonstrated for the evaluation and optimization of measurements of a large aero gas turbine engine. This shows that the instrument uncertainty is negligible in comparison to the amplifying effect of tooling and datum structures, although it should be noted that these effects scale the underlying instrument uncertainty. Before optimization the dominant source of uncertainty was the tooling design, after optimization the dominant source was thermal expansion of the engine; meaning that no further improvement can be made without measurement in a temperature controlled environment.

The engine measurements have shown that improvements in tooling design and tracker network configuration have the potential to reduce the combined uncertainty of engine measurements by a factor of 6. Following implementation of the recommendations into the production process gauge studies should be carried out to confirm this improvement and determine if additional sources of uncertainty related to the fit of the tooling are significant.

Acknowledgments

The research described herein has been carried out as part of the EPSRC, Light Controlled Factory Project (grant No. EP/K018124/1) at the Laboratory for Integrated Metrology Applications (LIMA) in the Department of Mechanical Engineering at the University of Bath. Thanks is also given to the consortium members in the LCF programme and in particular Rolls-Royce for support in this research.

References

[1] Peggs G N, Maropoulos P G, Hughes E B, Forbes A B, Robson S, Ziebart M and Muralikrishnan B 2009 Recent developments in large-scale dimensional metrology *Proc. Inst. Mech. Eng.* B **223** 571–95

[2] Muelaner J E, Martin O and Maropoulos P G 2011 Metrology enhanced tooling for aerospace (META): strategies for improved accuracy of jig built structures *SAE Aerotech* (Toulous: SAE International) available from: www.muelaner.com/part-to-part-assembly/tooling-for-aerospace/

[3] Muelaner J E, Kayani A, Martin O and Maropoulos P G 2011 Measurement assisted assembly and the roadmap to part-to-part assembly *7th Int. Conf. on Digital Enterprise Technology (Athens, 2011)* pp 11–9 Available from: www.muelaner.com/research/MADA/MAA_and_Roadmap_to_Part-To-Part.html

[4] Muelaner J E and Maropoulos P G 2008 Large scale metrology in aerospace assembly *5th Int. Conf. on Digital Enterprise Technology (Nantes, 2008)* pp 773–92 Available from: www.muelaner.com/measurement/large-scale-measurement/

[5] Kyle S 1999 Operational features of the Leica laser tracker *IEE Colloquium* pp 15–20

[6] Lau K, Hocken R J and Haight W C 1986 Automatic laser tracking interferometer system for robot metrology *Precis. Eng.* **8** 3–8

[7] Bhaumik P K 1988 Building aircraft assembly tools from a 3D database SAE Technical Paper 881428

[8] Burley G, Odi R, Naing S, Williamson A and Corbett J 1999 Jigless aerospace manufacture—the enabling technologies *Aerospace Manufacturing Technology Conf. and Exposition (Bellevue, Washington, 1999)* (Society of Automotive Engineers) Available from: http://papers.sae.org/1999-01-2286/

[9] Estler W T, Edmundson K L, Peggs G N and Parker D H 2002 Large-scale metrology—an update *CIRP Ann.-Manuf. Technol.* **51** 587–609

[10] BSI 1995 *General Metrology—Part 3: Guide to the Expression of Uncertainty in Measurement (GUM)* in PD 6461-3

[11] BSI 1999 *Geometrical Product Specifications (GPS)—Inspection by Measurement of Workpieces and Measuring Equipment—Part 1: Decision Rules for Proving Conformance or Non-Conformance with Specifications* in BS EN ISO 14253-1

[12] Anon 2010 *Measurement Systems Analysis* 4th edn (Southfield, MI: Auromotive Industry Action Group)

[13] Muelaner J E, Francis A J, Chappell M and Maropoulos P G 2015 A hybrid measurement systems analysis and uncertainty of measurement approach for industrial measurement in the light controlled factory *2nd Int. Conf. on Sustainable Design and Manufacturing (Seville, 2015)* Available from: www.muelaner.com/quality-assurance/hybrid-msa-and-uncertainty/

[14] Muralikrishnan B, Sawyer D, Blackburn C, Phillips S, Borchardt B and Estler W T 2009 ASME B89.4.19 performance evaluation tests and geometric misalignments in laser trackers *J. Res. Natl Inst. Stand. Technol.* **114** 21–35

[15] Clarke T A, Wang X, Cross N R, Forbes A B and Fossati P M 2001 Performance verification for large volume metrology systems *5th Int. Conf. on Laser Metrology, Machine Tool, CMM and Robot Performance, LAMDAMP (20 July 2001)* (Birmingham: WIT Press)

[16] Hughes B, Sun W, Forbes A and Lewis A 2010 Determining laser tracker alignment errors using a network measurement *CMSC (Reno, Nevada)* Available from: www.npl.co.uk/publications/determining-laser-tracker-alignment-errors-using-a-network-measurement

[17] ASME 2006 Performance evaluation of laser-based spherical coordinate measurement systems in B89.4.19

[18] Calkins J M 2002 Quantifying coordinate uncertainty fields in coupled spatial measurement systems *Mechanical Engineering* (Blacksburg: Virginia Polytechnic Institute and State University) p 226

[19] Forbes A B 2012 Weighting observations from multi-sensor coordinat measuring systems *Meas. Sci. Technol.* **23**

[20] Hughes B, Forbes A, Lewis A, Sun W, Veal D and Nasr K 2011 Laser tracker error determination using a network measurement *Meas. Sci. Technol.* **22** 045103

[21] FARO 2013 *FARO Vantage: Features, Benefits and Technical Specifications*

[22] Sandwith S and Predmore R 2001 Real-time 5-micron uncertainty with laser tracking interferometer systems using weighted trilateration *Boeing Large Scale Metrology Seminar (St. Louis, MO, 2001)*

[23] Triggs B, Mclauchlan P, Hartley R and Fitzgibbon A 1999 Bundle adjustment—a modern synthesis *Vision Algorithms: Theory and Practice, Int. Workshop on Vision Algorithms (Corfu, 1999)* Available from: http://lear.inrialpes.fr/pubs/2000/TMHF00/Triggs-va99.pdf

[24] Wang Z, Forbes A B and Maropoulos P G 2014 Laser tracker position optimization *J. Coordinate Metrology Systems Conf.* pp 8–12

[25] Phillips S D, Borchardt B, Estler W T and Buttress J 1998 Estimation of measurement uncertainty of small circular features measured by coordinate measuring machines *Precis. Eng.* **22** 87–97

[26] Joint Committee for Guides in Metrology 2007 *Evaluation of Measurement Data—Supplement 1 to the 'Guide to the Expression of Uncertainty in Measurement'—Propagation of Distributions Using a Monte Carlo Method*